

# Olfactory receptor neuron axon targeting: intrinsic transcriptional control and hierarchical interactions

Takaki Komiyama<sup>1</sup>, John R Carlson<sup>2</sup> & Liqun Luo<sup>1</sup>

From insects to mammals, olfactory receptor neurons (ORNs) expressing a common olfactory receptor target their axons to specific glomeruli with high precision. Here we show in *Drosophila* that the POU transcription factor *Acj6* controls the axon targeting specificity of a subset of ORN classes, as defined by the olfactory receptors that they express. Of these classes, some require *Acj6* cell-autonomously, whereas others require *Acj6* cell-nonautonomously. Mosaic analyses show that cooperative targeting occurs between axon terminals of the same ORN classes and that there are hierarchical interactions among different ORN classes. We propose that the precision of ORN axon targeting derives from both intrinsic transcriptional control and extensive axon-axon interactions.

Each class of ORNs in *Drosophila melanogaster* expresses 1–2 specific olfactory receptors<sup>1–5</sup> that presumably bind specific odorant molecules. ORNs target their axons to structures called glomeruli in the antennal lobe (equivalent to the vertebrate olfactory bulb) in a class-specific manner, thereby creating a spatial olfactory map in the brain<sup>3,4</sup>. In the glomeruli, ORN axons synapse with dendrites of their postsynaptic partners, projection neurons (equivalent to vertebrate mitral or tufted cells), most of which send dendrites to one specific glomerulus<sup>6</sup>. Projection neuron axons then relay specific olfactory information to higher brain centers<sup>7,8</sup>. This organizational logic is similar from flies to mammals<sup>9–12</sup>.

In mice, olfactory receptors themselves participate in ORN axon targeting<sup>11,13</sup>, but *Drosophila* olfactory receptors do not seem to have an axon targeting role<sup>5,14</sup>. The Src homology domain 2 (SH2)/SH3 adapter Dock<sup>15</sup>, the serine/threonine kinase Pak<sup>15</sup> and the cell surface proteins Dscam<sup>16</sup> and N-cadherin<sup>17</sup> are required for axon targeting by many, if not all, of the ORN classes that have been examined. Thus, although these molecules are essential components of ORN axon targeting, it is unclear whether they are used to distinguish among targets of different ORN classes or whether they are required more generally for all ORN classes. Different isoforms of Dscam are potential candidates for distinguishing among the targets of ORN classes, but this intriguing hypothesis has yet to receive experimental support. In addition, the Robo receptors have been implicated in the broad patterning of ORN axons<sup>18</sup>.

Here we show that the POU transcription factor *Acj6* is required for axon targeting by a specific subset of ORN classes. Of these ORNs, some classes require *Acj6* cell-autonomously, whereas others require *Acj6* nonautonomously. ORN axons of the same class tend to cluster together even when mistargeted, suggesting that there is cooperative targeting by axon terminals of the same ORN class (intra-class cooperativity). Nonautonomous mistargeting is caused by the presence of mutant ORNs of other classes (interclass interactions), and mosaic

analyses indicate that these interclass interactions are hierarchical. Thus, we propose that both intrinsic transcriptional control and extensive ORN-ORN interactions at the axon terminals contribute to precise ORN axon targeting.

## RESULTS

### *Acj6* is expressed in most postmitotic ORNs

We have previously shown that the POU transcription factors *Acj6* and *Drifter* are expressed in nonoverlapping sets of projection neurons in a lineage-specific fashion and that they regulate dendritic targeting of these projection neurons<sup>19</sup>. *Acj6* is also expressed in adult and developing olfactory sensory organs, the antenna and the maxillary palp<sup>1,20</sup>, raising the possibility that this transcription factor also controls ORN axon targeting.

We first confirmed and extended our previous expression studies. We found that *Acj6* is expressed in all ORNs in the antenna and most ORNs in the maxillary palp during development, and that *Acj6* is expressed only in postmitotic neurons (Fig. 1). By contrast, no ORNs in the antenna and very few in the maxillary palp express *Drifter* (see **Supplementary Fig. 1** online). In the studies reported below, we focused on the functions of *Acj6* in ORN axon targeting.

### Three categories of *acj6*-null phenotypes for 13 ORN classes

Because *acj6* is located on the X chromosome and null mutants are viable<sup>20,21</sup>, we studied 13 classes of ORNs (out of a total of about 40–50 in *Drosophila*) individually in hemizygous mutant males (*acj6*<sup>-</sup>/Y) and heterozygous female controls (*acj6*<sup>-/+</sup>). The boundaries of some glomeruli appeared less discrete in *acj6*<sup>-</sup>/Y as visualized by a general neuropil marker monoclonal antibody (mAb) nc82. This reduction in boundary definition occurred, at least in part, because a subset of projection neurons require *Acj6* for dendritic targeting<sup>19</sup>. Many glomeruli could, however, be identified. We visual-

<sup>1</sup>Department of Biological Sciences & Neurosciences Program, Stanford University, Stanford, California 94305, USA. <sup>2</sup>Department of Molecular, Cellular & Developmental Biology, Yale University, New Haven, Connecticut 06520, USA. Correspondence should be addressed to L.L. (lluo@stanford.edu).

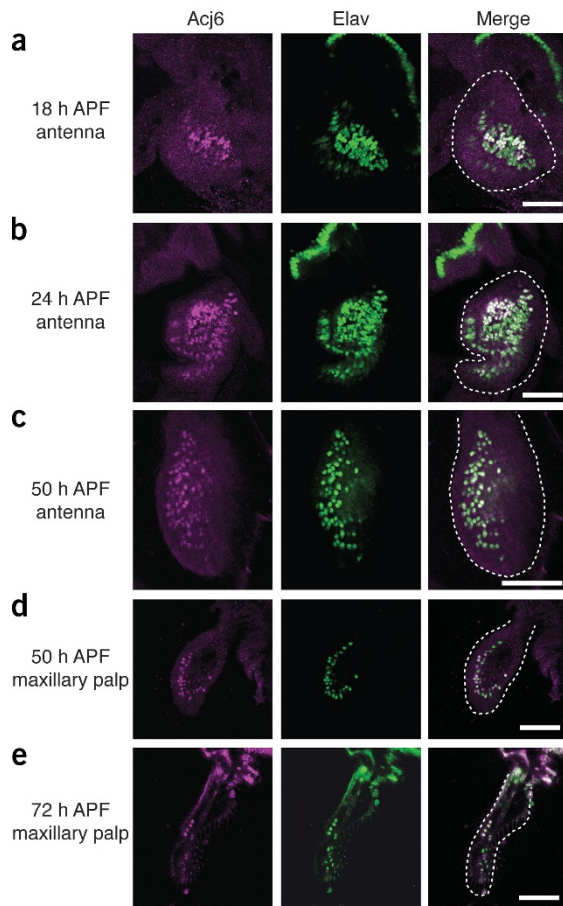


**Figure 1** *Acj6* is expressed in developing ORNs. (a–c) At 18 h APF (a), *Acj6* is expressed in a large subset of postmitotic ORNs defined by expression of the pan-neural postmitotic marker *Elav* in the developing third antennal segment (outlined in images on right; the cells outside the outlines are not ORNs); at 24 and 50 h APF (b,c), *Acj6* seems to be expressed in all *Elav*-positive ORNs. (d,e) At both 50 and 72 h APF, *Acj6* is expressed in most ORNs in the developing maxillary palp (outlined in images on right).

ized axon targeting by specific ORN classes by using OR-Gal4 drivers (promoters of individual ORs drive expression of the yeast transcription factor Gal4; see Methods) to drive the expression of a membrane-targeted form of green fluorescent protein (mCD8-GFP), which allowed visualization of ORN axon targeting to specific glomeruli counterstained with nc82.

The *acj6*-null mutant phenotypes could be divided into three categories (Table 1). In the first category (Or22a, Or42a, Or46a and Or92a),

mCD8-GFP expression was not detected in *acj6* mutant antennal lobes (data not shown) or in olfactory sensory organs (Fig. 2). This observation is consistent with the previous finding that a subset of ORNs requires *Acj6* for olfactory receptor expression<sup>1</sup> and therefore these OR-Gal4 drivers are inactive in *acj6* mutants. These classes were excluded from further analyses because we do not have *Acj6*-independent class-specific markers with which to examine their axon targeting.

In the second category (Or47b, Or85e and Or88a), ORN axon targeting was normal in *acj6* mutant flies (Fig. 3). Of these classes, Or85e-Gal4 seemed to have lower expression in *acj6* mutant flies as compared with wild type, although the axon projection pattern was still visible. Because most ORNs also send axons to the same glomerulus in the contralateral antennal lobe<sup>3,4</sup>, we tested whether contralateral targeting by these ORNs was affected by examining axon projections in the brain 10 d after excising one antenna (which allows ORN axons from the excised antenna to degenerate). We observed normal targeting to the same glomeruli on both ipsi- and contralateral sides (Supplementary Fig. 2 online).

In the third category (Or43a, Or47a, Or59c, Or71a, Or83c and Gr21a), ORN axons did not target appropriately. Although in each case ORN axons entered the antennal lobe, they spread over a larger region, sometimes including the appropriate area, and often formed ectopic clusters (Figs. 4b,i,p and 5b,j,q; compare with Figs. 4a,h,o and 5a,i,p). We observed almost identical targeting defects when we used the presynaptic marker *n-syb*-GFP<sup>22</sup>, suggesting that the ectopic clusters represent synaptic terminals rather than *en passant* axons (Supplementary Fig. 3 online).

### *Acj6* functions in ORNs for their axon targeting

This above analysis of ‘whole-fly’ mutants showed that *Acj6* is required for axon targeting of a specific subset of ORN classes. To determine where in the olfactory system *Acj6* functions for proper

**Table 1** ORN axon targeting data and *Acj6* expression in corresponding projection neurons

| ORN class | Olfactory organ | <i>acj6</i> <sup>+/+</sup> | <i>acj6</i> <sup>-/-</sup> | eyFlp        | hsFlp        | eyFlp reverse | <i>Acj6</i> in PN |
|-----------|-----------------|----------------------------|----------------------------|--------------|--------------|---------------|-------------------|
| Or22a     | AT              | DM2                        | –                          |              |              |               | No                |
| Or42a     | MP              | VM7                        | –                          |              |              |               | Yes               |
| Or46a     | MP              | VA5                        | –                          |              |              |               | No                |
| Or92a     | AT              | VA2                        | –                          |              |              |               | Yes               |
| Or47b     | AT              | VA1Im                      | VA1Im (9/9)                |              |              |               | Yes               |
| Or85e     | MP              | VC1                        | VC1 (7/7)                  |              |              |               | No                |
| Or88a     | AT              | VA1d                       | VA1d (10/10)               |              |              |               | Yes               |
| Or59c     | MP              | 1                          | def. (5/5)                 | def. (9/10)  | 1 (9/9)      | def. (13/13)  | Yes               |
| Or71a     | MP              | VC2                        | def. (11/12)               | def. (8/10)  | VC2 (9/9)    | def. (10/14)  | No                |
| Gr21a     | AT              | V                          | def. (8/8)                 | def. (11/12) | V (37/42)    | def. (8/12)   | ND                |
| Or43a     | AT              | DA4                        | def. (7/7)                 | def. (5/5)   | def. (10/10) | DA4 (13/13)   | ND                |
| Or47a     | AT              | DM3                        | def. (7/7)                 | def. (4/4)   | def. (4/4)   | DM3 (18/19)   | ND                |
| Or83c     | AT              | VA6 (+DA3)                 | def. (6/6)                 | def. (10/10) | def. (8/8)   | VA6 (7/7)     | Yes               |

PN, projection neuron; ‘yes’, partner PNs express *Acj6*; ‘no’, partner PNs do not express *Acj6*; ND, not determined; def., defective; –, OR-Gal4 not expressed in hemizygote (see text); AT, third antennal segment; MP, maxillary palp. Data in the last column are from ref. 19 or inferred from ref. 8. See ref. 19 for a functional study in projection neurons. Numbers of examples of the described phenotypes are shown in parentheses.

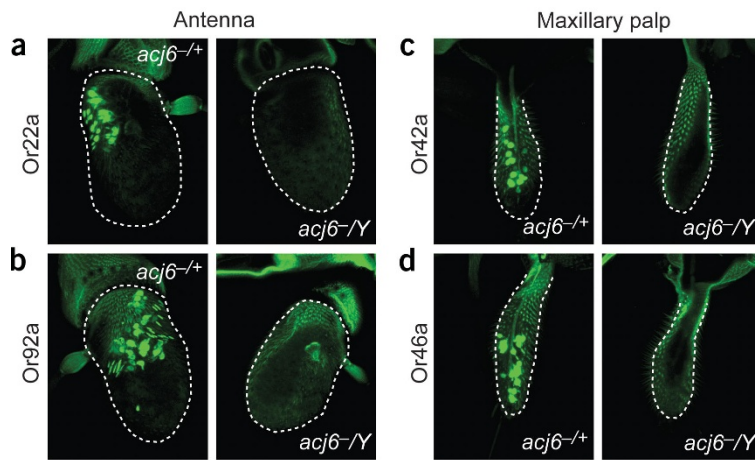


**Figure 2** Some OR-Gal4 drivers are not expressed in *acj6* mutant ORNs. (a–d) The OR-Gal4 drivers of Or22a (a), Or92a (b), Or42a (c) and Or46a (d) are expressed in heterozygous (*acj6*<sup>-/+</sup>) controls (left) but not in hemizygous (*acj6*<sup>-/Y</sup>) mutants (right). UAS-mCD8GFP was used as a marker. The third antennal segment (a,b) and the maxillary palp (c,d) are outlined.

ORN axon targeting, we carried out mosaic analyses using the MARCM system (mosaic analysis with a repressible cell marker)<sup>23</sup> on all six classes that showed defects in the whole-fly mutant analysis (Table 1), using Flp recombinase driven by the *eyeless* promoter (*eyFlp*)<sup>24</sup>. *eyFlp* induces mitotic recombination in the antenna and maxillary palp but not in the central brain<sup>16</sup>, which renders 30–50% of all ORNs homozygous mutant for *acj6*, while all neurons in the central brain, including projection neurons, remain heterozygous (ref. 16; and T.K., D. Berdnik and L.L., unpublished data). It was formally possible that *eyFlp* might create mutant clones of non-neuronal cells in the brain but, because *Acj6* expression in the brain is restricted to postmitotic neurons in all developmental stages examined<sup>19</sup>, we consider that loss of *Acj6* expression in non-neuronal cells should have no effect on phenotype.

All six classes examined in this *eyFlp* MARCM analysis had axon targeting defects (Figs. 4d,k,r and 5d,l,s; compare with Figs. 4c,j,q and 5c,k,r) that were very similar to the whole-fly mutant phenotypes. Because the glomerular morphology in the *eyFlp* experiment was similar to that of the wild type, these data ruled out the possibility that the axon targeting defects in whole-fly *acj6* mutants were secondary to a general disruption of antennal lobe patterning. In addition, because *Acj6* expression was restricted to postmitotic neurons in the antenna and maxillary palp (Fig. 1), we conclude that the ORN axon targeting phenotypes are caused by a lack of *Acj6* in ORNs.

### Evidence for intraclass cooperativity

As in the whole-fly mutants, mutant ORN axon terminals in *eyFlp* experiments tended to form distinct clusters in the antennal lobe

(arrows in Figs. 4d,k,r and 5d,l,s) rather than to spread diffusely; these phenotypes suggested that there was cooperative targeting by axons of ORNs of the same class even when the axons were mistargeted (intraclass cooperativity). We quantified clusters of axon terminals both at the correct targets and at ectopic locations in each brain (two antennal lobes; Fig. 6a).

Wild-type clones had two correct clusters (with the exception of the Or83c class; Fig. 6) and no ectopic clusters, whereas mutant clones of all six classes showed significant numbers of ectopic clusters in addition to or instead of clusters in their correct glomeruli. Notably, we did not observe extensive axon fasciculation among ORNs of the same class, in either the wild type or the mutants, before the axons reached their target (Supplementary Fig. 4 online), and the ectopic clusters were strongly labeled by presynaptic marker *n-syb*-GFP (Supplementary Fig. 3 online). Thus, the clusters

are likely to represent cooperative axon targeting by ORNs of the same class at the level of synaptic terminals rather than at the level of axon paths.

### Cell-autonomous and -nonautonomous ORN classes

To test the cell autonomy of the *Acj6* requirement, we generated small MARCM clones by using heat-shock promoter-driven Flp recombinase (*hsFlp*) and by inducing clones late in larval development. Usually 0–2 cells were labeled by each OR-Gal4 driver in each hemisphere, and therefore the number of *acj6*<sup>-/Y</sup> ORNs was much smaller than that observed by *eyFlp* MARCM. We found that Or43a, Or47a

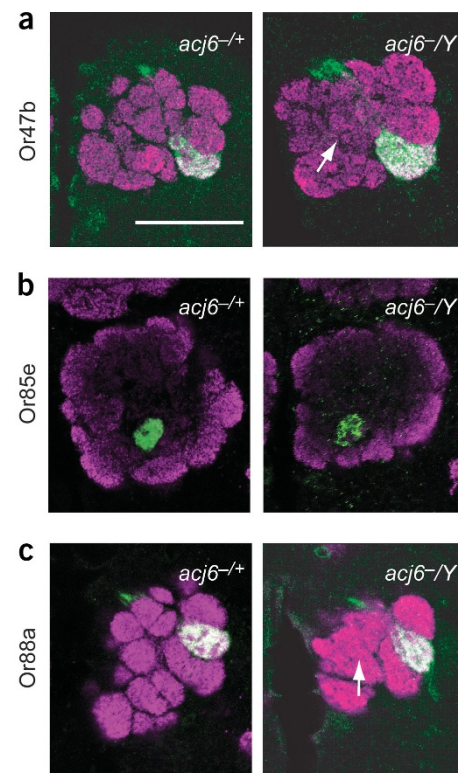


**Figure 3** Some ORN classes do not require *Acj6* for axon targeting. (a–c) Or47b (a), Or85e (b) and Or88a (c) ORNs target their axons to glomeruli VA1Im, VC1 and VA1d, respectively, in both heterozygous controls (*acj6*<sup>-/+</sup>, left) and hemizygous mutants (*acj6*<sup>-/Y</sup>, right). Expression of Or85e-Gal4 is weak in hemizygous (b, right) as compared with heterozygous (b, left) flies. Arrows indicate less-discrete glomerular boundaries. All images in this and subsequent figures are confocal z-stacks (either full or partial) oriented with dorsal up; either the right hemisphere is shown with the midline to the left, or both hemispheres are shown with the midline indicated by a broken line. Green indicates mCD8-GFP, magenta indicates mAb nc82. Scale bar, 50 μm.

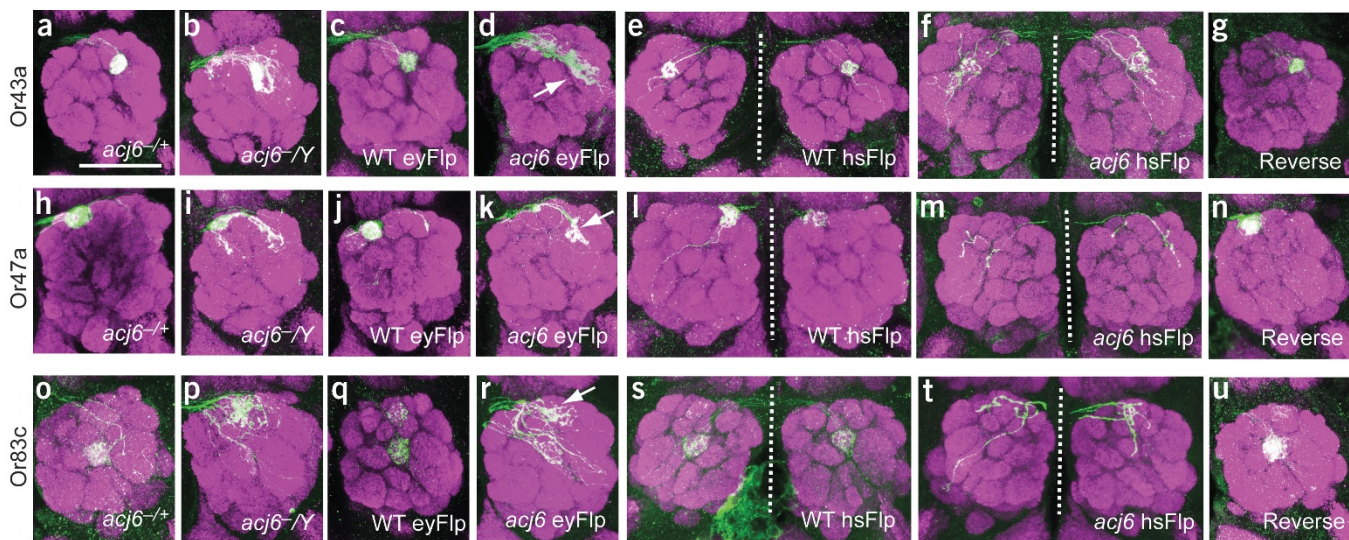


**Figure 4** Some ORN classes require *Acj6* cell-autonomously for axon targeting. (a–f) Or43a ORNs target glomerulus DA4 in *acj6* heterozygous controls (a), but have defective projections in *acj6* hemizygous mutants (b). eyFlp *acj6*<sup>-/-</sup> (d) and hsFlp *acj6*<sup>-/-</sup> (f) clones also have defective projections as compared with their wild-type control (c,e), showing a cell-autonomous requirement of *Acj6*. (h–m) Or47a ORNs target glomerulus DM3 in *acj6* heterozygous, wild-type eyFlp and hsFlp MARCM controls (h,i,l), but have defective projections in *acj6* hemizygous mutants (j), eyFlp MARCM (k) and hsFlp MARCM (m). (o–t) Or83c ORNs target glomerulus VA6, and sometimes another glomerulus (DA3) weakly, in *acj6* heterozygous, wild-type eyFlp and hsFlp MARCM controls (o,q,s), but have defective projections in *acj6* hemizygous mutants (p), eyFlp MARCM (r) and hsFlp MARCM (t). Reverse eyFlp MARCM experiments show normal targeting for these three classes (g,n,u). Arrows in d,k and r indicate ectopic clusters of axon terminals. Dotted lines indicate the midline.

and Or83c showed a phenotype qualitatively similar to that seen on eyFlp MARCM: individual axon branches and terminals were distributed over a large area of the antennal lobe (Fig. 4f,m,t; compare with 4e,l,s). These data indicate that the mistargeting phenotypes of these three classes are cell-autonomous. By contrast, Or59c, Or71a and Gr21a axons targeted correctly in hsFlp MARCM (Fig. 5g,n,u; compare with 5f,m,t), indicating that these three classes do not require *Acj6* cell-autonomously for axon targeting and that the defects observed in whole-fly and eyFlp MARCM experiments were caused by an *Acj6* requirement in other cells.

What is the source of cell-nonautonomous mistargeting of Or59c, Or71a and Gr21a? Perdurant of *Acj6* protein from progenitor cells in small hsFlp clones is unlikely because *Acj6* was detected only in post-mitotic ORNs (Fig. 1). The difference between the eyFlp MARCM and the hsFlp MARCM strategies was that many more ORNs were mutant for *acj6* in eyFlp MARCM than in hsFlp MARCM. Thus, the axon mistargeting of these three classes was probably caused by mutant ORNs of other classes. This model of interclass interactions received further support from the fact that in rare cases where only one labeled Or59c cell was *acj6*<sup>-/-</sup> in eyFlp MARCM, the axon of this single mutant cell was still mistargeted (Fig. 5e). In these cases, all of the other Or59c neurons were *acj6*<sup>-/+</sup> or wild type (*acj6*<sup>+/+</sup>); thus, the mistargeting of the single *acj6*<sup>-/-</sup> Or59c ORN must have been caused by the presence of unlabeled mutant ORNs of other classes.

### Interclass interactions are hierarchical

To investigate further this interclass interaction model, we used a reverse MARCM strategy in which only homozygous wild-type cells were labeled (Methods). With eyFLP, 30–50% of all ORNs were *acj6*<sup>-/-</sup> but not visualized; only the siblings of mitotic recombination that were wild type could be visualized by specific OR-Gal4 drivers in the presence of unlabeled mutant ORNs. As predicted from our

model, wild-type axons of the three nonautonomous classes showed targeting defects (Fig. 5h,o,v; Table 1) analogous to those in ‘forward’ eyFlp MARCM (Fig. 5d,l,s). Thus, correct targeting of these ORNs requires *Acj6* function in other ORNs. By contrast, reverse MARCM analysis showed normal targeting for the three classes that required *Acj6* cell-autonomously (Fig. 4g,n,u; Table 1); these wild-type ORNs were able to target correctly in spite of mistargeting of other ORNs, including mutant ORNs of their own classes.

There are several implications from the reverse MARCM analyses. First, these observations confirm that the mistargeting phenotypes of Or43a, Or47a and Or83c are cell-autonomous, whereas those of Or59c, Or71a and Gr21a are cell-nonautonomous. Second, the different results in eyFLP MARCM and eyFLP reverse MARCM experiments for the three autonomous classes rule out the possibility, at least for these three classes, that the intraclass interaction is responsible for axon targeting defects; in other words, the mutant axons do not ‘drag’ their wild-type counterparts of these classes to cause them to mistarget.

Third, these results indicate that the interclass interactions are hierarchical—the nonautonomous classes depend on classes that require *Acj6* autonomously for their axon targeting, but the autonomous classes are not affected by mistargeting of autonomous or nonautonomous ORNs. Thus, the autonomous classes seem to be higher in the hierarchy (more independent) than the nonautonomous classes. This hierarchical interaction model also explains the three ORN classes that target normally in *acj6* whole-fly mutants (Or47b, Or85e and Or88a, Fig. 3): these classes depend neither on *Acj6* nor on interactions with other ORNs that are affected in *acj6* mutants. It remains to be determined whether these ‘unaffected’ or ‘autonomous’ classes can target independently of any other ORN classes, or whether they depend on other ORN classes that are not affected in the *acj6* mutant.

Notably, the autonomous and nonautonomous classes of ORNs were distinct in the nature of their mistargeting. We quantified

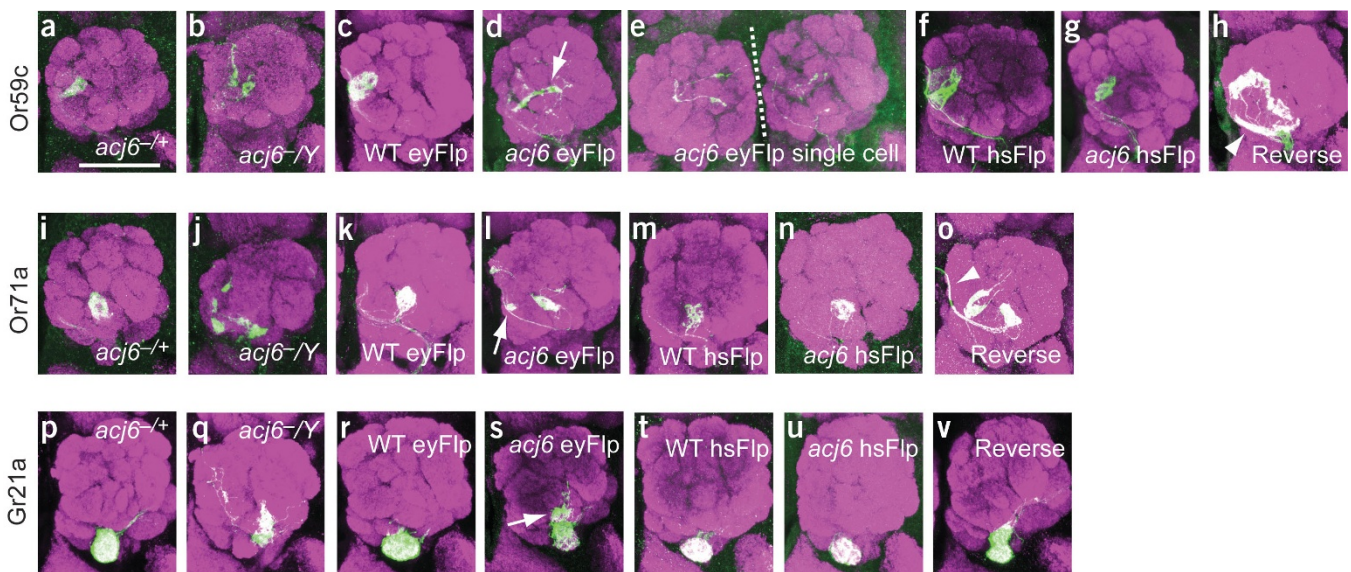


**Figure 5** Some ORN classes require *Acj6* cell-nonautonomously for axon targeting. (**a–g**) Or59c ORNs target glomerulus 1 in *acj6* heterozygous, wild-type eyFlp and hsFlp MARCM controls (**a,c,f**), but have defective projections near glomerulus 1 in *acj6* hemizygous mutants (**b**). *acj6*<sup>-/-</sup> clones in eyFlp MARCM also have defective projections (**d**), even when only a single cell is labeled in the whole brain (**e**;  $n = 2$ ; in the example shown, the single labeled ORN axon enters through the right antennal lobe). By contrast, in hsFlp MARCM, where fewer total ORNs are mutant for *acj6*, the axons target glomerulus 1 correctly (**g**). (**i–n**) Or71a ORNs target glomerulus VC2 in *acj6* heterozygous, wild-type eyFlp and hsFlp MARCM controls (**i,k,m**), but have defective projections near VC2 in *acj6* hemizygous mutants (**j**). *acj6*<sup>-/-</sup> clones in eyFlp MARCM also have defective projections (**l**), but in hsFlp MARCM the axons target VC2 correctly (**n**). (**p–u**) Gr21a ORNs target glomerulus V in *acj6* heterozygous, wild-type eyFlp and hsFlp MARCM controls (**p,r,t**), but have defective projections near V in *acj6* hemizygous mutants (**q**). *acj6*<sup>-/-</sup> clones in eyFlp MARCM also have defective projections (**s**), but in hsFlp MARCM the axons target V correctly (**u**). These classes show mistargeting in reverse eyFlp MARCM (**h,o,v**) similar to ‘forward’ eyFlp MARCM phenotypes. Arrowheads in **h** and **o** indicate axon tracts, not mistargeted axon terminals. Arrows in **d**, **l** and **s** indicate clusters of axon terminals.

targeting frequency to the correct glomeruli and to six zones that were most often mistargeted by each of the six ORN classes (Fig. 6b). This analysis showed that mistargeting was stereotypical. For autonomous classes, most often axons did not invade the correct glomeruli and ectopic clusters frequently formed far away from the correct glomeruli (for example, Or43a or Or83c). These observations indicate that coarse axon targeting by these classes is altered by the loss of *Acj6* functions in these ORNs. For nonautonomous classes, however, axon targeting usually included the correct target, and ectopic clusters were located adjacent to the correct target, indicating that ORN-ORN interactions may be used to locally refine targeting specificity of these ORNs.

## DISCUSSION

We have identified a transcription factor, *Acj6*, that controls ORN axon targeting. *Acj6* controls axon targeting by a specific subset of ORNs cell-autonomously. Combinations of transcription factors including *Acj6* should presumably determine the intrinsic targeting specificity of ORNs by controlling the expression of cell surface molecules that steer ORN growth cones. Future studies should identify these molecules and shed light on the molecular mechanisms underlying precise axon targeting of ORNs.

Because *Acj6* is required in a subset of both ORNs and projection neurons for, respectively, their axonal and dendritic targeting specificity in the antennal lobe, an attractive possibility is that *Acj6* controls the specificity of connections between pre- and postsynaptic neurons that are destined to synapse with each other. This ‘matching’ scheme by transcription factors has been proposed in the vertebrate spinal cord circuit<sup>25,26</sup>. Our study of 13 ORN classes argues against this possibility (Table 1). For example, of the classes that do not

require *Acj6* cell-autonomously, Or47b, Or59c and Or88a target glomeruli innervated by dendrites of *Acj6*-positive projection neurons, whereas Or71a and Or85e target glomeruli innervated by *Acj6*-negative projection neurons.

The lack of matching could be explained if both ORNs and projection neurons possess substantial self-organizing properties in their targeting, which would reduce the requirement of specific recognitions between ORNs and their partner projection neurons. Indeed, we have previously shown that, before ORN axon arrival, dendrites of projection neurons have already created a prototypic map in the antennal lobe, likely through projection neuron dendrite-dendrite interactions<sup>27,28</sup>. Furthermore, on the basis of this study, we propose that ORNs also have self-organizing capabilities that rely on axon-axon interactions among ORNs, as discussed below.

## Axon-axon interactions

In addition to the intrinsic transcriptional program that is likely to be used to specify coarse targeting, our genetic mosaic analyses implicate the presence of extensive ORN-ORN interactions that might help to refine local targeting by positioning axon terminals relative to each other. Axon terminals of the same ORN classes show cooperativity to achieve convergent targeting (intra-class cooperativity), as shown by the significant clustering of axon terminals of the same ORN class even when the axons were mistargeted. This could be mediated by homophilic adhesion between axon terminals of the same ORN classes. Notably, similar intra-class cooperativity has been implicated in mice, and olfactory receptors seem to contribute to this cooperativity<sup>29–31</sup>.

We have also shown that ORNs of different classes show hierarchical interactions (interclass interactions), implying that different ORN

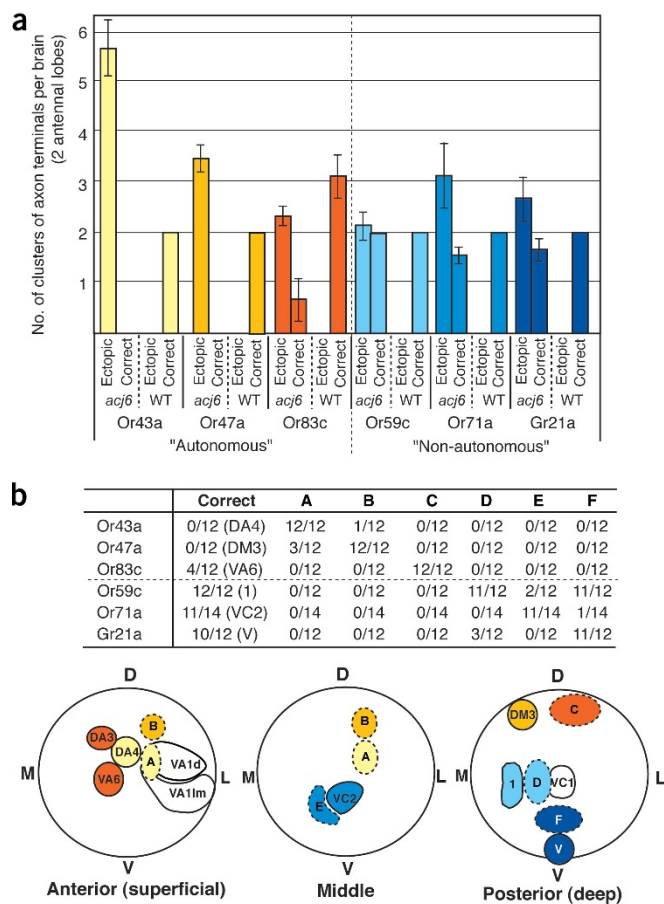


**Figure 6** Quantitative analysis of mistargeting defects in *eyFlp* MARCM. (a) Number of axon terminal clusters at ectopic and correct targets per brain (two antennal lobes). Or43a, Or47a and Or83c have ectopic clusters, but rarely have clusters in the correct targets in *acj6*<sup>-/-</sup> clones, whereas Or59c, Or71a and Gr21a almost always have clusters in the correct targets in addition to ectopic clusters. Wild-type Or83c ORNs target VA6 invariably and sometimes also DA3 weakly, giving an average of about 3.1 clusters at correct targets ( $n = 7$  for Or71a *acj6* and Or83c wild type;  $n = 6$  for other genotypes). Error bars indicate the s.e.m. (b) Mistargeting is stereotypical. Six small zones (labeled A–F) are most frequently mistargeted by each of the six ORN classes. Zone A, medial quarter of DA1 and its posterior adjacent; B, medial quarter of VA1d and VA11m, and its posterior adjacent; C, DL1 and DL5; D, lateral adjacent of 1; E, medial and ventral adjacent of VC2; F, dorsal adjacent to V. Top, zones A–F are most frequently mistargeted by Or43a, Or47a, Or83c, Or59c, Or71a and Gr21a, respectively, but they are rarely mistargeted by other classes. Bottom, location of glomeruli and zones A–F in the antennal lobe (the three-dimensional antennal lobe is represented by three circles at different z planes). White glomeruli are innervated by Or47b, Or85e and Or88a, the three classes that are not affected in *acj6* hemizygous mutants. D, dorsal; V, ventral; L, lateral; M, medial.

classes use different strategies for axon targeting. How could *acj6* mutant ORNs (autonomous classes) affect the targeting of other ORNs (nonautonomous classes)? Because disruption of the interclass interactions results in local mistargeting (Fig. 6b), such interactions probably act locally in the antennal lobe. In principle, mutant axons could affect other axons indirectly, for example, by inducing defects in dendrites of target neurons that in turn affect targeting of other axons. It has been shown, however, that mistargeted projection neuron dendrites do not affect targeting of partner ORN axons<sup>28</sup>. Thus,

we favor the possibility that ORN axons of different classes directly interact with each other.

One scheme could be that pioneering axons of some classes are used as either attractive or repulsive cues by later-innervating axons. Indeed, two of the three nonautonomous classes that we identified are ORNs in the maxillary palp (Or59c and Or71a), whereas all three autonomous classes are ORNs in the antenna (Table 1); at least some axons from the antenna reach the developing antennal lobe well before any axons from the maxillary palp<sup>27</sup>. A rigorous test of this timing hypothesis requires future identification of class-specific markers expressed early in development; the OR-Gal4 drivers used in this study are switched on too late (Methods) to facilitate studies of the early development of ORN axons in a class-specific manner.

Axon-axon interaction has been proposed to regulate axon patterning and wiring specificity in several other systems<sup>32–34</sup>. Superimposed on the intrinsic targeting specificity of each ORN controlled by *Acj6* and other transcription factors, we propose that the intraclass cooperativity and interclass interactions identified in this study contribute significantly to ensure the precise targeting of about 50 ORN classes to about 50 glomerular targets in the *Drosophila* antennal lobe, and perhaps of a much larger number of ORN classes to their glomerular targets in the mammalian olfactory bulb.

## METHODS

**OR-Gal4 drivers.** The OR-Gal4 drivers were generated by using the promoters of olfactory receptor genes to direct expression of the yeast transcription factor Gal4. OR-Gal4 fusions for the following receptors have been described: Or47a<sup>3</sup>, Or47b<sup>3</sup>, Or22a<sup>5</sup>, Or43a<sup>14</sup>, Or59c<sup>16</sup>, Gr21a<sup>35</sup>. Additional OR-Gal4 fusions for the receptors Or42a, Or46a, Or92a, Or85e, Or88a, Or71a and Or83c were made by similar strategies (C. Warr, A. Goldman, C. Miller, D. Lessing, A. Ray, and R. Ignell; unpublished data; details available from J.R.C. on request). For all classes examined, the onset of olfactory receptor expression during development was significantly later than 50 h after puparium formation (APF), a time point after the completion of major targeting events. Thus, although OR-Gal4 drivers are excellent markers for examining class-specific axon targeting in adults, they are not suitable for descriptive studies or transgenic manipulations during development.

**Mosaic analyses.** We carried out MARCM analyses as described<sup>23</sup>. In short, the mutation *acj6* and the Gal4 repressor Gal80 were placed *trans*-heterozygous to each other. Flp-mediated recombination created homozygous *acj6* cells that had lost Gal80 and were therefore labeled by the Gal4-UAS system. The genotype was *TubP-Gal80, eyFlp* (or *hsFLP*), *FRT19A/acj6*, *FRT19A/OR-Gal4/UAS-mCD8GFP* (or *UAS-nsybGFP*). For *hsFlp* MARCM, late third-instar larvae were heat shocked for 1 h at 37 °C. For reverse MARCM, Gal80 and *acj6* were placed on the same chromosome arm, and recombination created both homozygous wild-type cells that had lost Gal80 and were therefore labeled and unlabeled cells homozygous for *acj6* and Gal80. The genotype was *eyFlp, FRT19A / TubP-Gal80, acj6*, *FRT19A/OR-Gal4/UAS-mCD8GFP*. Fixation, immunostaining and imaging were done as described<sup>6,19</sup>.

It should be noted that although all labeled cells were homozygous mutant (or wild type) in the MARCM (or reverse MARCM) strategy, only a small subset of homozygous cells (those expressing a particular OR-Gal4) were labeled.

Note: Supplementary information is available on the Nature Neuroscience website.

## ACKNOWLEDGMENTS

We thank L. Vosshall, K. Scott, C. Warr, A. Goldman, C. Miller, D. Lessing, A. Ray and R. Ignell for the OR-Gal4 drivers; E. Buchner for antibodies; and T. Clandinin, K. Shen and members of the Luo laboratory for comments on the manuscript. This work was supported by grants from the US National Institutes of Health (to L.L. and J.R.C.).

## COMPETING INTERESTS STATEMENT

The authors declare that they have no competing financial interests.

Received 21 June; accepted 28 June 2004

Published online at <http://www.nature.com/natureneuroscience/>

1. Clyne, P.J. *et al.* A novel family of divergent seven-transmembrane proteins: candidate odorant receptors in *Drosophila*. *Neuron* **22**, 327–338 (1999).
2. Vosshall, L.B., Amrein, H., Morozov, P.S., Rzhetsky, A. & Axel, R. A spatial map of olfactory receptor expression in the *Drosophila* antenna. *Cell* **96**, 725–736 (1999).
3. Vosshall, L.B., Wong, A.M. & Axel, R. An olfactory sensory map in the fly brain. *Cell* **102**, 147–159 (2000).
4. Gao, Q., Yuan, B. & Chess, A. Convergent projections of *Drosophila* olfactory neurons to specific glomeruli in the antennal lobe. *Nat. Neurosci.* **3**, 780–785 (2000).
5. Dobritsa, A.A., van der Goes van Naters, W., Warr, C.G., Steinbrecht, R.A. & Carlson, J.R. Integrating the molecular and cellular basis of odor coding in the *Drosophila* antenna. *Neuron* **37**, 827–841 (2003).
6. Jefferis, G.S.X.E., Marin, E.C., Stocker, R.F. & Luo, L. Target neuron prespecification in the olfactory map of *Drosophila*. *Nature* **414**, 204–208 (2001).
7. Marin, E.C., Jefferis, G.S.X.E., Komiyama, T., Zhu, H. & Luo, L. Representation of the glomerular olfactory map in the *Drosophila* brain. *Cell* **109**, 243–255 (2002).
8. Wong, A.M., Wang, J.W. & Axel, R. Spatial representation of the glomerular map in the *Drosophila* protocerebrum. *Cell* **109**, 229–241 (2002).
9. Vassar, R. *et al.* Topographic organization of sensory projections to the olfactory bulb. *Cell* **79**, 981–991 (1994).
10. Ressler, K.J., Sullivan, S.L. & Buck, L.B. Information coding in the olfactory system: evidence for a stereotyped and highly organized epitope map in the olfactory bulb. *Cell* **79**, 1245–1255 (1994).
11. Mombaerts, P. *et al.* Visualizing an olfactory sensory map. *Cell* **87**, 675–686 (1996).
12. Zou, Z., Horowitz, L.F., Montmayeur, J.P., Snapper, S. & Buck, L.B. Genetic tracing reveals a stereotyped sensory map in the olfactory cortex. *Nature* **414**, 173–179 (2001).
13. Wang, F., Nemes, A., Mendelsohn, M. & Axel, R. Odorant receptors govern the formation of a precise topographic map. *Cell* **93**, 47–60 (1998).
14. Wang, J.W., Wong, A.M., Flores, J., Vosshall, L.B. & Axel, R. Two-photon calcium imaging reveals an odor-evoked map of activity in the fly brain. *Cell* **112**, 271–282 (2003).
15. Ang, L.H., Kim, J., Stepensky, V. & Hing, H. Dock and Pak regulate olfactory axon pathfinding in *Drosophila*. *Development* **130**, 1307–1316 (2003).
16. Hummel, T. *et al.* Axonal targeting of olfactory receptor neurons in *Drosophila* is controlled by Dscam. *Neuron* **37**, 221–231 (2003).
17. Hummel, T. & Zipursky, S.L. Afferent induction of olfactory glomeruli requires N-cadherin. *Neuron* **42**, 77–88 (2004).
18. Jhaveri, D., Saharan, S., Sen, A. & Rodrigues, V. Positioning sensory terminals in the olfactory lobe of *Drosophila* by Robo signaling. *Development* **131**, 1903–1912 (2004).
19. Komiyama, T., Johnson, W.A., Luo, L. & Jefferis, G.S.X.E. From lineage to wiring specificity. POU domain transcription factors control precise connections of *Drosophila* olfactory projection neurons. *Cell* **112**, 157–167 (2003).
20. Clyne, P.J. *et al.* The odor specificities of a subset of olfactory receptor neurons are governed by Acj6, a POU-domain transcription factor. *Neuron* **22**, 339–347 (1999).
21. Ayer, R.K., Jr. & Carlson, J. acj6: a gene affecting olfactory physiology and behavior in *Drosophila*. *Proc. Natl. Acad. Sci. USA* **88**, 5467–5471 (1991).
22. Estes, P.S., Ho, G.L., Narayanan, R. & Ramaswami, M. Synaptic localization and restricted diffusion of a *Drosophila* neuronal synaptobrevin–green fluorescent protein chimera in vivo. *J. Neurogenet.* **13**, 233–255 (2000).
23. Lee, T. & Luo, L. Mosaic analysis with a repressible cell marker for studies of gene function in neuronal morphogenesis. *Neuron* **22**, 451–461 (1999).
24. Newsome, T.P., Asling, B. & Dickson, B.J. Analysis of *Drosophila* photoreceptor axon guidance in eye-specific mosaics. *Development* **127**, 851–860 (2000).
25. Arber, S., Ladle, D.R., Lin, J.H., Frank, E. & Jessell, T.M. ETS gene *Er81* controls the formation of functional connections between group Ia sensory afferents and motor neurons. *Cell* **101**, 485–498 (2000).
26. Lin, J.H. *et al.* Functionally related motor neuron pool and muscle sensory afferent subtypes defined by coordinate ETS gene expression. *Cell* **95**, 393–407 (1998).
27. Jefferis, G.S.X.E. *et al.* Developmental origin of wiring specificity in the olfactory system of *Drosophila*. *Development* **131**, 117–130 (2004).
28. Zhu, H. & Luo, L. Diverse functions of N-cadherin in dendritic and axonal terminal arborization of olfactory projection neurons. *Neuron* **42**, 63–75 (2004).
29. Ebrahimi, F.A. & Chess, A. Olfactory neurons are interdependent in maintaining axonal projections. *Curr. Biol.* **10**, 219–222 (2000).
30. Vassalli, A., Rothman, A., Feinstein, P., Zapotocky, M. & Mombaerts, P. Minigenes impart odorant receptor-specific axon guidance in the olfactory bulb. *Neuron* **35**, 681–696 (2002).
31. Feinstein, P. & Mombaerts, P. A contextual model for axonal sorting into glomeruli in the mouse olfactory system. *Cell* **117**, 817–831 (2004).
32. Clandinin, T.R. & Zipursky, S.L. Afferent growth cone interactions control synaptic specificity in the *Drosophila* visual system. *Neuron* **28**, 427–436 (2000).
33. Wang, J., Zugates, C.T., Liang, I.H., Lee, C.H. & Lee, T. *Drosophila* Dscam is required for divergent segregation of sister branches and suppresses ectopic bifurcation of axons. *Neuron* **33**, 559–571 (2002).
34. Ng, J. *et al.* Rac GTPases control axon growth, guidance and branching. *Nature* **416**, 442–447 (2002).
35. Scott, K. *et al.* A chemosensory gene family encoding candidate gustatory and olfactory receptors in *Drosophila*. *Cell* **14**, 661–673 (2001).